environmental microbiology

Environmental Microbiology (2014) **16**(8), 2525–2537 doi:10.1111/1462-2920.12393

Halorhabdus tiamatea: proteogenomics and glycosidase activity measurements identify the first cultivated euryarchaeon from a deep-sea anoxic brine lake as potential polysaccharide degrader

Johannes Werner,[1,2†] Manuel Ferrer,[3†] Gurvan Michel,[4] Alexander J. Mann,[1,2] Sixing Huang,[1] Silvia Juarez,[5] Sergio Ciordia,[5] Juan P. Albar,[5] María Alcaide,[3] Violetta La Cono,[6] Michail M. Yakimov,[6] André Antunes,[7] Marco Taborda,[8] Milton S. da Costa,[9] Tran Hai,[10] Frank Oliver Glöckner,[1,2] Olga V. Golyshina,[10] Peter N. Golyshin[10*‡] and Hanno Teeling[1‡]: The MAMBA Consortium

[1]*Max Planck Institute for Marine Microbiology, Bremen, Germany.*
[2]*Jacobs University Bremen gGmbH, Bremen, Germany.*
[3]*Institute of Catalysis, CSIC, Madrid, Spain.*
[4]*UPMC University Paris 6 and CNRS, UMR 7139 Marine Plants and Biomolecules, Station Biologique, Roscoff, Bretagne, France.*
[5]*Proteomic Facility, CNB-National Centre for Biotechnology, CSIC, Madrid, Spain.*
[6]*Laboratory of Marine Molecular Microbiology, Institute for Coastal Marine Environment (IAMC), CNR, Messina, Italy.*
[7]*Institute for Biotechnology and Bioengineering (IBB), Centre of Biological Engineering, Micoteca da Universidade do Minho, University of Minho, Braga, Portugal.*
[8]*Microbiology Unit, BIOCANT Biotechnological Park, Cantanhede, Portugal.*
[9]*Department of Life Sciences, University of Coimbra, Coimbra, Portugal.*
[10]*School of Biological Sciences, Bangor University, Bangor, Gwynedd, UK.*

Summary

Euryarchaea from the genus *Halorhabdus* have been found in hypersaline habitats worldwide, yet are represented by only two isolates: *Halorhabdus utahensis* AX-2^T from the shallow Great Salt Lake of Utah, and *Halorhabdus tiamatea* SARL4B^T from the Shaban deep-sea hypersaline anoxic lake (DHAL) in the Red Sea. We sequenced the *H. tiamatea* genome to elucidate its niche adaptations. Among sequenced archaea, *H. tiamatea* features the highest number of glycoside hydrolases, the majority of which were expressed in proteome experiments. Annotations and glycosidase activity measurements suggested an adaptation towards recalcitrant algal and plant-derived hemicelluloses. Glycosidase activities were higher at 2% than at 0% or 5% oxygen, supporting a preference for low-oxygen conditions. Likewise, proteomics indicated quinone-mediated electron transport at 2% oxygen, but a notable stress response at 5% oxygen. *Halorhabdus tiamatea* furthermore encodes proteins characteristic for thermophiles and light-dependent enzymes (e.g. bacteriorhodopsin), suggesting that *H. tiamatea* evolution was mostly not governed by a cold, dark, anoxic deep-sea habitat. Using enrichment and metagenomics, we could demonstrate presence of similar glycoside hydrolase-rich *Halorhabdus* members in the Mediterranean DHAL Medee, which supports that *Halorhabdus* species can occupy a distinct niche as polysaccharide degraders in hypersaline environments.

Received 4 April, 2013; accepted 5 January, 2014. *For correspondence. E-mail p.golyshin@bangor.ac.uk; Tel. +44 1248 38 3629; Fax +44 1248 37 0731. †These authors contributed equally to this work. ‡These authors contributed equally to this work.

Introduction

Hypersaline habitats are found worldwide, for example in the form of terrestrial and deep-sea brine lakes or man-made solar salterns. The salinities of these habitats range from just above seawater to salt saturation, and their salt compositions range from concentrated seawater with sodium chloride as major salt (thalassohaline habitats) to compositions where other salts such as magnesium chloride dominate (athalassohaline habitats). Despite harsh conditions, microorganisms inhabit hypersaline habitats with a spectrum from species that merely tolerate hypersalinity to true halophiles that require 0.5–2.5 M of salt for growth (Andrei *et al.*, 2012).

Two major strategies have evolved to cope with high salinities and prevent enzymes from denaturing and salt-out precipitation (Galinski, 1995). The first, the organic osmolyte strategy, consists of countering high osmolarities by intracytoplasmic accumulation of compatible solutes like quaternary amines or sugars such as trehalose. The second, the salt-in strategy, relies on accumulation of high levels of internal potassium (and to lesser extents sodium) chloride.

Among the most peculiar hypersaline habitats are deep-sea brine lakes, like the Orca Basin in the Northern Gulf of Mexico (Pilcher and Blumstein, 2007), the ice-sealed Antarctic Vida lake (Murray *et al*., 2012), the numerous deep-sea hypersaline anoxic lakes (DHALs) in the Eastern Mediterranean Sea (Bortoluzzi *et al*., 2011) and the Red Sea (Antunes *et al*., 2011a). The thalassohaline DHAL Shaban Deep in the Red Sea was discovered in 1984 (Pautot *et al*., 1984), and since several novel species were isolated from this location (Antunes *et al*., 2003; 2007; 2008a,b). *Halorhabdus tiamatea* SARL4B^T stems from the brine–sediment interface of the Shaban Deep's Eastern basin (26°13.9′ N, 35°21.3′ E, −1447 m depth, pH 6.0, salinity: 244) and features pleomorphic, non-pigmented cells that grow chemoorganoheterotrophically under anoxic to micro-oxic conditions [optimum: 45°C; pH 5.6–7.0; 27% NaCl (w/v)], but poorly under oxic conditions (Antunes *et al*., 2008a). The only other *Halorhabdus* (*Hrd.*) (Oren *et al*., 2007) species with a validly published name so far is *Halorhabdus utahensis* AX-2^T (DSM 12940^T), a sediment isolate from the southern arm of the shallow thalassohaline Great Salt Lake in Utah, USA (Wainø *et al*., 2000). *Halorhabdus utahensis* also features pleomorphic but pigmented cells that can grow under anoxic and oxic conditions (Table 1). Both *Hrd.* species exhibit a 16S ribosomal RNA (rRNA) sequence identity of 99.3% (Fig. 1). The genome of

Table 1. General characteristics of the *H. tiamatea* and *H. utahensis* genomes.

	H. tiamatea	*H. utahensis*
Contigs	1 chromosome, 1 plasmid	1 chromosome
Chromosome size (G + C content)	2 815 791 bp (63.4%)	3 116 795 bp (62.9%)
Plasmid size (G + C content)	330 369 bp (57.4%)	–
Total genes (coding density)	3023 (83.2%)	2998 (86.2%)
Genes with annotated functions	1974 (65.3%)	2243 (74.8%)
rRNAs	3 (one rRNA operon)	3 (one rRNA operon)
tRNAs	46 (all 20 amino acids)	45 (all 20 amino acids)

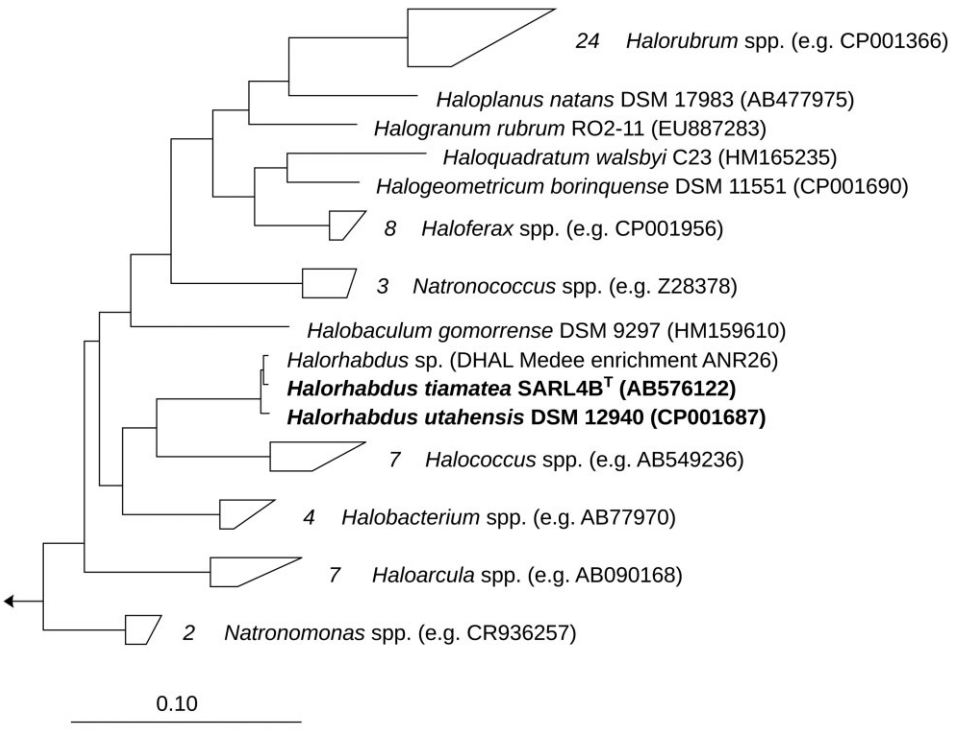

Fig. 1. Maximum likelihood tree of the family *Halobacteriaceae.* The tree was calculated with RAxML v. 7.0.3 (Stamatakis *et al*., 2005) with *Methanospirillum hungatei* JF-1 as outgroup. The scale bar represents 10% estimated sequence divergence.

H. utahensis has been completely sequenced (Anderson *et al*., 2009), whereas until now only a draft sequence was available for *H. tiamatea* (Antunes *et al*., 2011b). Both genomes share a large proportion of genes, but also exhibit notable niche differentiations, such as an increased number of genes for membrane transport and utilization of maltose, maltodextrin, phosphonate, and di- and oligopeptides in *H. tiamatea* (Antunes *et al*., 2011b). *Halorhabdus tiamatea* and *H. utahensis* belong to those *Halobacteriaceae* species that can degrade plant polysaccharides (Anderson *et al*., 2011). For instance, *H. utahensis* has proven β-xylanase, β-xylosidase (Wainø and Ingvorsen, 2003) and cellulase activities (Zhang *et al*., 2011).

We sequenced and closed the *H. tiamatea* genome *de novo*, annotated it manually and analysed its niche adaptations with an emphasis on polysaccharide degradation and response to oxygen. This included in-depth phylogeny-based annotations of its carbohydrate-active enzymes (CAZymes), corresponding glycosidase activity measurements and proteome analyses of *H. tiamatea* cultures grown in liquid media under 0%, 2% and 5% of oxygen-containing headspace.

Results and discussion

Genome features

The genome of *H. tiamatea* (Fig. 2A and B) consists of a 2.8 Mbp chromosome and a putative 330 kbp plasmid with 2743 and 280 predicted genes respectively (Table 1). The chromosome exhibits high overall collinearity with the *H. utahensis* chromosome, but differs by multiple larger inversions and minor genome rearrangements (Supporting Information Fig. S1). Conversely, the putative *H. tiamatea* plasmid exhibits no such collinearity, and mostly harbours hypothetical and conserved hypothetical genes as well as genes for transposases, DNA-associated proteins and restriction enzymes. The transposase density of the putative plasmid is 12.5% whereas it is only ~ 2% for the *H. tiamatea* chromosome. The chromosome furthermore features three regions with putative phage genes that are characterized by dissimilar tetranucleotide usage patterns (Fig. 2A). *Halorhabdus tiamatea*, like *H. utahensis*, contains one clustered regularly interspaced short palindromic repeats (CRISPR) element (*H. tiamatea*: 4703 bp with 71 spacers; *H. utahensis*: 3381 bp with 51 spacers).

Monosaccharide utilization

Halorhabdus tiamatea can degrade hexoses via the semi-phosphorylated Entner–Doudoroff (ED) pathway. Resulting D-glyceraldehyde-3-phosphate can be further oxidized to pyruvate via the lower part of the Embden–Meyerhof–Parnas (EMP) pathway. The upper part lacks 6-phosphofructokinase. Instead the genome encodes a 1-phosphofructokinase that is co-located with a fructose-1,6-bisphosphate aldolase gene. Such incompleteness or variations of the EMP and gluconeogenesis pathways are common in *Archaea*. Gluconeogenesis has been deemed non-operational in *H. utahensis* because of a lack of pyruvate phosphate dikinase (Anderson *et al*., 2011), which in *H. tiamatea* is also not present. *Halorhabdus tiamatea* has the potential to use fructose by conversion to fructose-1,6-bisphosphate (1-phosphofructokinase), and galactose via the Leloir pathway.

The pentose-5-phosphate (PP) pathway in *H. tiamatea* is missing the oxidative branch, but the non-oxidative branch is present. The latter is likely used to convert pentoses to fructose-6-phosphate. Without the PP pathway's oxidative branch, glucose cannot be converted to ribulose-5-phosphate. However, both *Hrd.* genomes harbour genes to convert xylose and arabinose to ribulose-5-phosphate. *Halorhabdus tiamatea* has a ribokinase that *H. utahensis* lacks, which implies that *H. tiamatea* in contrast to *H. utahensis* can also utilize ribose.

Polysaccharide utilization

Both *Hrd.* species contain high numbers of CAZyme genes, i.e. genes for enzymes that synthesize, modify or breakup glycosides (Henrissat and Coutinho, 2001). *Halorhabdus tiamatea* SARLB^T has in total 50 glycoside hydrolase genes (15.9 GHs Mbp^{-1}), 42 on its chromosome and eight on its putative plasmid (Supporting Information Table S1) – the highest numbers so far observed in *Archaea* (Supporting Information Fig. S2). *Halorhabdus utahensis* has 44 GH genes (14.1 GHs Mbp^{-1}) according to the CAZy database as of 10 December 2013 (Cantarel *et al*., 2009; Lombard *et al*., 2013).

Halorhabdus tiamatea features genes for the degradation of xylan, arabinan, arabinoxylan and galactan-containing hemicelluloses, pectin and likely cellulose. These polysaccharides occur in land plant cell walls, algae (Popper *et al*., 2011) and seagrass [e.g. pectin in *Zostera marina* (Zaporozhets, 2003; Khotimchenko *et al*., 2012)]. *Halorhabdus tiamatea* furthermore has the genomic potential to degrade exogenous storage carbohydrates such as sucrose or α-1,4-glucans [e.g. starch (Antunes *et al*., 2008a) or glycogen].

Xylans can be hydrolysed to xylose by concerted action of seven GH10 endo-β-1,4-xylanases and three GH43 β-xylosidases. A dedicated transporter can subsequently import the xylose monomers. Arabinans can be cleaved to L-arabinose by concerted action of a GH43 endo-α-1,5-L-arabinosidase and six GH51 exo-acting α-L-arabinofuranosidases. The latter can also remove

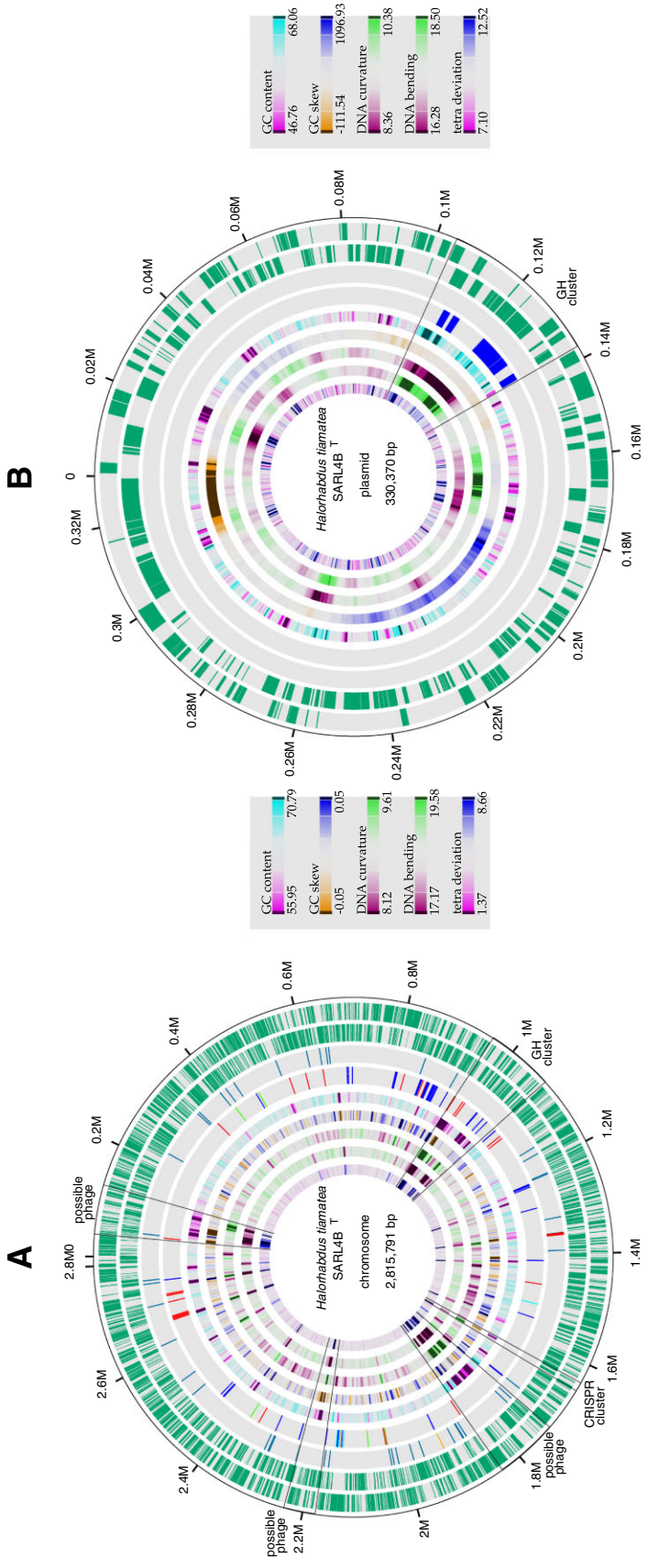

Fig. 2. Circular representation of the (A) chromosome and (B) plasmid of *H. tiamatea*. From inside to outside: GC content, GC skew, DNA curvature, DNA bending, deviation from the average tetranucleotide composition, CAZymes (blue: glycoside hydrolase, red: glycosyl transferase, green: carbohydrate esterase, orange: polysaccharide lyase, cyan: carbohydrate binding module), RNAs (red: rRNA, green: tRNA, orange: other RNA), genes in reverse direction and genes in forward direction. GC content and GC skew were calculated with a self-written PERL script (sliding windows: 5 kbp for chromosome; 0.5 kbp for plasmid). DNA curvature and bending were calculated with the program banana from the EMBOSS package (Rice *et al.*, 2000). TETRA (Teeling *et al.*, 2004) was used for the calculation of the deviation from the average tetranucleotide composition (sliding windows: 5 kbp for chromosome; 1 kbp for plasmid).

Table 2. Glycoside hydrolases in the *Hrd.* genomes.

	H. tiamatea	*H. utahensis*
GH2	4 (1.27), **3**	4 (1.28)
GH3	6 (1.91), **4**	7 (2.25)
GH4	1 (0.32), **1**	2 (0.64)
GH5	2 (0.64)	7 (2.25)
GH9	1 (0.32)	1 (0.32)
GH10	7 (2.22), **4**	4 (1.28)
GH11	0 (0.00)	2 (0.64)
GH13	7 (2.22), **6**	1 (0.32)
GH31	1 (0.32), **1**	0 (0.00)
GH32	2 (0.64)	0 (0.00)
GH42	1 (0.32)	0 (0.00)
GH43	3 (0.95), **2**	4 (1.28)
GH51	6 (1.91), **1**	1 (0.32)
GH67	1 (0.32), **1**	1 (0.32)
GH77	1 (0.32), **1**	1 (0.32)
GH88	1 (0.32)	0 (0.00)
GH93	1 (0.32)	0 (0.00)
GH94	3 (0.95)	2 (0.64)
GH95	1 (0.32)	1 (0.32)
GH97	1 (0.32)	1 (0.32)

GH abundances in the genomes of *H. tiamatea* and *H. utahensis* (according to the CAZy database as of 10 December 2013). The first number represents absolute counts, the number in parentheses counts per Mbp and numbers in boldface GHs detected in proteome data.

decorating L-arabinose side chains from arabinoxylans and arabinogalactans. Arabinoxylans are likely degraded by concerted action of GH10 xylanases and GH51 arabinosidases. The resulting L-arabinose is then likely taken up, isomerized to L-ribulose and subsequently funnelled into the PP pathway. *Halorhabdus tiamatea* lacks any obvious galactanase and thus probably cannot use the backbones of galactans and arabinogalactans. However, its genome codes for a GH4 α-galactosidase and a GH42 β-galactosidase, which likely enable *H. tiamatea* to cleave galactose side chains from hemicelluloses (Popper *et al*., 2011).

The *H. tiamatea* genome encodes a single PL1 family polysaccharide lyase with pectate lyase function, and a GH88 enzyme. The latter resembles the d-4,5-unsaturated β-glucuronyl hydrolase from *Bacillus* sp. GL1, which participates in the hydrolysis of unsaturated glycosaminoglycan oligosaccharides released by glycosaminoglycan lyases (Itoh *et al*., 2004). Similarly, the *H. tiamatea* GH88 likely cleaves unsaturated oligopectins released by its PL.

Like *H. utahensis*, *H. tiamatea* has a modular GH9 with a C-terminal family 3 carbohydrate-binding module. This architecture resembles the endo-processive cellulase E4 from *Thermomonospora fusca* (Sakon *et al*., 1997). Two GH5 enzymes with possible glucanase functions could provide complementary cellulolytic activity. Released oligoglucans may be further degraded by GH3 β-glucosidases. Alternatively, resulting cellobiose dimers might be processed by two GH94 cellobiose phosphorylases with inorganic phosphate to glucose and glucose-1-phosphate (Yernool *et al*., 2000). A third GH94 gene (HTIA_1257) is highly similar to laminaribiose phosphorylase from *Paenibacillus* sp. YM1 (Kitaoka *et al*., 2012). Thus, even though *H. tiamatea* lacks obvious laminarinases, it still may be able to use exogenous laminaribioses.

Halorhabdus tiamatea has a putative maltose transporter and is known to grow on maltose (Antunes *et al*., 2008a). This disaccharide results from degradation of exogenous starch or glycogen by action of maltogenic GH13 enzymes (Supporting Information Fig. S3) and can be subsequently hydrolysed into two α-D-glucose units. Sucrose is another disaccharide that *H. tiamatea* can potentially use because of presence of a GH32 β-fructosidase, which cleaves sucrose to glucose and fructose.

Both sequenced *Hrd.* species are particularly rich in GH10 xylanases and GH43 β-xylosidases (*H. utahensis*: 4× GH10, 4× GH43; *H. tiamatea*: 7× GH10, 3× GH43). Other polysaccharide-degrading enzymes are abundant in both species as well (Table 2), for instance GH2 (e.g. β-mannosidase and β-glucuronidase) and GH3 (β-glucosidase). However, their CAZyme repertoires also exhibit differences, as for example GH32 (β-fructofuranosidase) was only found in *H. tiamatea*. Likewise, GH13 genes are notably more frequent in *H. tiamatea* than in *H. utahensis* (7 vs 1). Conversely, *H. utahensis* has more GH5 genes (7 vs 2), one with proven cellulase activity (Zhang *et al*., 2011).

A peculiarity of *H. tiamatea* is that most of its arabinan-degradation genes are encoded on its putative plasmid as a single cluster of four GH51 exo-acting α-N-arabinofuranosidases and a L-arabinose isomerase, whereas the complementing GH43 endo-α-1,5-L-arabinosidase is encoded by its chromosome. The GH cluster on the putative plasmid as well as one large GH cluster on the chromosome have dissimilar tetranucleotide usage patterns that stand out even above those of the three putative phage-infected regions (Fig. 2A and B). This indicates that the capacity for the degradation of some polysaccharides might have been laterally acquired. Extensive lateral acquisition of genes is common in *Halobacteria* and likely played a major role in their evolution from anaerobic methanogens (Nelson-Sathi *et al*., 2012).

Fermentations

Halorhabdus tiamatea relies on fermentations under anoxic conditions (see Supporting Information Text). It has a four-subunit pyruvate : ferredoxin oxidoreductase for pyruvate oxidation, allowing disposal of reducing equivalents by hydrogen release. Indeed, *H. tiamatea* encodes a

cytoplasmic heterotetrameric [Ni-Fe] hydrogenase, which agrees with the finding that *H. tiamatea* produces gas from sugars (Antunes *et al*., 2008a).

Sulphur stimulates growth of *H. utahensis* and is reduced to hydrogen sulphide. It has been suggested that this is facilitated fermentation rather than respiration that serves as hydrogen sink without producing energy (Wainø *et al*., 2000). Conversely, sulphur reduction has not been reported for *H. tiamatea* (Antunes *et al*., 2008a), and its genome does not seem to contain any respective genes. The bidirectional tetrameric hydrogenase (I) might be able to reduce sulphur as shown in *Pyrococcus furiosus* (Ma *et al*., 1993; 2000), but this has not been observed in *H. tiamatea*.

Halorhabdus tiamatea produces acids when grown on maltose (Antunes *et al*., 2008a) and is known to possess an L-lactate dehydrogenase (Antunes *et al*., 2011b) and an L-lactate permease, likely for lactate export. Besides, *H. tiamatea* also features a D-lactate dehydrogenase. Lactate fermentation seems to be the sole mechanism for recycling of reduced pyridine and flavin adenine dinucleotides under anoxic conditions. Acetate is a second likely fermentation product as the *H. tiamatea* genome encodes an AMP-forming acetyl-CoA synthetase, whose reverse reaction releases acetate from acetyl-CoA while conserving energy as ATP.

Halorhabdus tiamatea has all genes for anaerobic glycerol degradation: a glycerol kinase and an anaerobic glycerol-3-phosphate dehydrogenase (*glpABC*) (Rawls *et al*., 2011). In *Escherichia coli*, the anaerobic oxidation of glycerol-3-phosphate to dihydroxyacetone phosphate by GlpABC is coupled to the reduction of fumarate to succinate (Schryvers and Weiner, 1981), but other halophilic archaea such as representatives of the genera *Haloferax* and *Haloarcula* have been shown to metabolize glycerol under anoxic conditions to D-lactate, acetate and pyruvate (Oren and Gurevich, 1994).

Krebs cycle

Halorhabdus tiamatea has a complete Krebs cycle (without glyoxylate shunt). The only anaplerotic reaction seems to be the carboxylation of phosphoenolpyruvate (PEP) by PEP carboxylase. *Halorhabdus tiamatea* features a malate : quinone-oxidoreductase that funnels electrons directly in the quinone pool and a ferredoxin-dependent 2-oxoglutarate oxidoreductase. Both enzymes might facilitate to run the Krebs cycle in reverse from oxaloacetate to the precursor 2-oxoglutarate, as in some methanogenic archaea (Sakai *et al*., 2011). The malate : quinone-oxidoreductase could operate reversely in terms of thermodynamics, as has been discussed for *Helicobacter pylori* (Kather *et al*., 2000). *Halorhabdus tiamatea* lacks a distinct fumarate reductase such as the membrane-bound type found in *E. coli* or the coenzyme M-reducing cytoplasmic type found in many methanogenic archaea; hence, a reverse Krebs cycle would involve the regular succinate dehydrogenase.

Respiration

Halorhabdus tiamatea grows under hypoxic, but poorly under oxic conditions (Antunes *et al*., 2008a). Its genome encodes all genes for the archaeal membrane-bound NADH : ubiquinone oxidoreductase, as well as cytochrome bd and bc ubiquinol oxidase subunits, a complete 3-subunit copper-containing cytochrome oxidase, together with cytochrome c biogenesis and copper transport genes, and a V-type ATPase.

It is known that *H. tiamatea* reduces nitrate and nitrite (Antunes *et al*., 2008a). However, its genome does not encode any membrane-associated (Nar) or periplasmic (Nap) respiratory nitrate reductase. It also lacks a membrane-bound Nrf-type cytochrome c nitrite reductase as it is typically found in anaerobes employing dissimilatory nitrate reduction to ammonium. *Halorhabdus tiamatea* does possess genes for a Nir-type cytoplasmic nitrite reductase, which, however, is non-respiratory as it typically acts only as an electron sink to cope with excess reductants under anoxic conditions. Nir activity is strictly anaerobic and if constitutively required might contribute to the oxygen sensitivity of *H. tiamatea*.

It is not clear whether respiration of endogenous fumarate produced by carboxylation of PEP to oxaloacetate via a reversely operating Krebs cycle is functional. However, exogenous fumarate can likely be reduced to succinate as in other halophilic archaea (Oren, 1991).

Response to oxygen

Proteomics on extracts of *H. tiamatea* cultures grown under three oxygen conditions (0%, 2% and 5% in the culture headspace) revealed an increasing stress response with increasing oxygen exposure. Of 699 identified proteins (~ 24% of the cytosolic proteome), 435 were quantified using a label-dependent method, with at least two peptides in triplicate experiments (Supporting Information Table S2). Compared with the anoxic condition, expression ratios (O_2/anoxic) varied from 0.36 to 5.22-fold at 2% oxygen, and from below 0.01 to 10.19-fold at 5% oxygen. The 2% oxygen condition caused a mild response with induction of six (including a catalase) and repression of two proteins with at least ± twofold changes. The 5% oxygen condition caused a more pronounced shift in the protein expression pattern, with higher abundances of 32 (7.0%) and lower abundances of 38 (8.4%) proteins. Notably expressed were a catalase (7.5-fold), a superoxide dismutase (6.8-fold), a thiosulfate-

sulfurtransferase-like rhodanese (4.9-fold) likely for scavenging oxidative thiyl-radicals (Remelli *et al*., 2012), a thioredoxin reductase (2.7-fold) probably with antioxidant functions and a chlorite dismutase (2.4-fold) counteracting oxidative hypochlorite. In contrast, expression of the chaperonine Hsp20 was more than 100-fold lower at 5% oxygen than at the anoxic condition.

The energy metabolism was down-regulated at the 5% oxygen condition, most notably subunits of the pyruvate : ferredoxin oxidoreductase (> 100-fold), which seemed to act as major regulation unit for controlling the intracellular carbon flux, but also enzymes from the semi-phosphorylated ED (2.0-fold) and lower EMP pathways (up to 2.3-fold), the Krebs cycle (up to 4.0-fold) and a putative hydrogenase component (3.6-fold). Likewise, most subunits of the NADH-quinone dehydrogenase were down regulated (up to 2.5-fold).

Almost half (24/50) of the glycoside hydrolases (3× GH2, 4× GH3, 1× GH4, 4× GH10, 6× GH13, 1× GH31, 2× GH43, 1× GH51, 1× GH67 and 1× GH77) as well as three polysaccharide deacetylases were identified, which stresses their relevance. The 5% oxygen condition led to a down-regulation of six GHs (2× GH10, 3× GH13 and 1× GH31 ranging from 2.2 to 3.9-fold), including the trehalose synthase. Additional GHs seemed to be down-regulated, albeit with a lower than twofold change in expression ratio. Likewise, a subunit of the maltose transporter was down regulated (> 100-fold).

Glucosidase activities

We tested hydrolysis of 18 *p*-nitrophenol (*p*NP) glycosides with *H. tiamatea* protein extracts from the above-mentioned three oxygen conditions with and without 3 M KCl. Glucosidase activities were not detected for three *p*NP glycosides (α-maltose, α-xylose and β-arabinose) and positive for the remaining 15 (Fig. 3). The latter support that *H. tiamatea* can utilize α-glucans (starch, amylose and amylopectin), β-glucans (cellulose), β-xylans, arabinans and galactose-containing hemicelluloses, as suggested by the genome analysis. Activity was also positive for *p*NP glycosides of the typical plant saccharides α-fucose, α-rhamnose and α-mannose, as well as for β-lactose.

Total activity was highest for the 2% and lowest for the 5% oxygen condition, which agrees with the proteome experiments and supports an adaptation towards micro-oxic conditions (Fig. 3A). Individual activities varied with salt and oxygen concentrations, indicating that *H. tiamatea* actively regulates its sugar metabolism.

Alpha-arabinose activity was positive, and a GH51 α-L-arabinofuranosidase (located on the putative plasmid) was expressed in the proteome experiments. This conflicts with previous findings that *H. tiamatea* does not grow

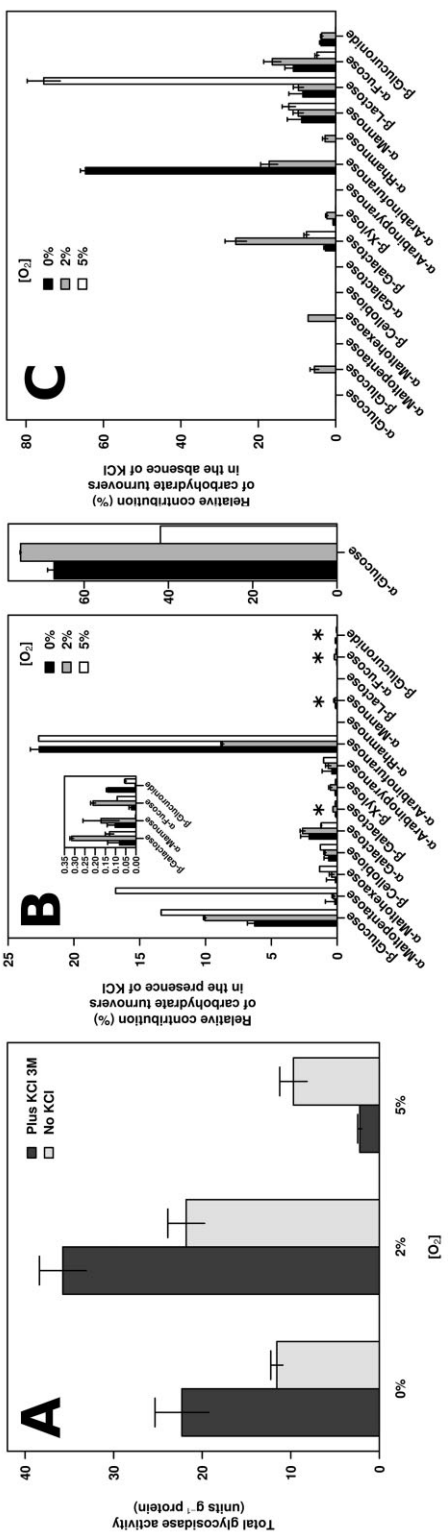

Fig. 3. Glucosidase activity measurements in *H. tiamatea* cell extracts with *p*NP sugar derivatives: (A) total glycosidase activity (units/mg total protein), (B) relative proportion of glycosidase activities in reaction mixtures containing 3 M KCl and (C) relative proportion of glycosidase activities in reaction mixtures without 3 M KCl. Note: In B, sugars marked by an asterisk are shown in the inset and α-glucose in a dedicated panel on the right, each at separate scales.

on arabinose (Antunes *et al*., 2008a). Such discrepancies among genomic potential, functional assays and growth experiments are common. For instance, it is known that sugar oligomers rather than monomers induce genes for polysaccharide degradation in *Flavobacteria* (Martens *et al*., 2011). Hence, growth experiments with monomers might constitute an artificial situation for polymer degraders under which they do not exhibit their normal *in situ* physiology.

Light-dependent enzymes

Some halobacteria use light-driven ion pumps: bacteriorhodopsin as a proton pump for chemiosmotic ATP generation and halorhodopsin for importing chloride against the concentration gradient. *Halorhabdus tiamatea* has two genes with rhodopsin domains, one bacteriorhodopsin-like gene and 10 genes containing the bacterio-opsin activator domain (including one located on the putative plasmid). Both rhodopsin domain proteins have the R-X-X-D proton acceptor and D-X-X-X-K retinal Schiff-base binding sites (Jiao *et al*., 2006). One of these genes likely has a sensory function, as it is co-located with a methyl-accepting chemotaxis signal transducer gene (see Supporting Information Text for motility). The second rhodopsin gene is co-located with genes encoding the bacteriorhodopsin-like protein, one of the bacterio-opsin activator domain proteins, two isoprenoid biosynthesis enzymes (likely for the retinal cofactor) and the exinuclease subunit UvrA. It is noteworthy that the genome encodes not only the complete UvrABC DNA repair system, but also the blue light-dependent deoxyribodipyrimidine photolyase (Park *et al*., 1995), both of which repair ultraviolet-induced DNA damages.

Traits associated with a thermophilic lifestyle

As many other halophilic archaea, both *Hrd.* species share traits that are typically associated with a thermophilic lifestyle. Both feature a four-subunit pyruvate : ferredoxin oxidoreductase, which is usually found in hyperthermophilic anaerobes (Mai and Adams, 1996) and in methanogenic archaea, many of which are also moderately thermophilic. In addition, the known β-xylanases, β-xylosidase and cellulase of *H. utahensis* feature remarkably high temperature optima of 55/70°C, 65°C and 70°C (3 M NaCl) respectively (Wainø and Ingvorsen, 2003; Zhang *et al*., 2011). Both species also feature surprisingly high optimum growth temperatures [*H. utahensis*: 50°C (Wainø *et al*., 2000); *H. tiamatea*: 45°C (Antunes *et al*., 2008a)]. Likewise, both species harbour a gene for LysW, an enzyme that bypasses thermolabile diaminopimelate in lysine biosynthesis in *Thermus thermophilus* and hyperthermophilic *Archaea* (Horie *et al*., 2009).

Storage compounds and osmoregulation

Halorhabdus tiamatea is known to produce poly-β-hydroxy-alkanoates (PHA) (Antunes *et al*., 2008a). A class III PHA synthase is encoded by clustered *phaE* and *phaC* genes, and likely forms short-chained polymers with up to five carbon moieties in the hydroxyacyl backbone. Some bacteria are known to build a membrane complex from poly-β-hydroxy-butyrate, polyphosphate and calcium ions. This complex is believed to function as a calcium/phosphate symporter (Reusch and Sadoff, 1988) and if present in *H. tiamatea* might take part in osmoregulation.

Halorhabdus tiamatea also encodes a family 35 glycosyltransferase (GT) glycogen phosphorylase and a GH77 α-1,4-glucanotransferase. Both are essential for endogenous glycogen usage. However, *H. tiamatea* lacks known enzymes for *de novo* glycogen biosynthesis, i.e. a glycogen synthase (GT3 or GT5) or glycogen branching enzyme (GH13). This suggests that *H. tiamatea* either uses unknown isofunctional enzymes or employs a novel pathway for internal α-1,4-glucan biosynthesis. A possible candidate is a GH13 gene (HTIA_0925) with high similarity to the amylosucrase from *Neisseria polysaccharea* (Supporting Information Fig. S3). The latter can build an internal storage α-1,4 glucan by simultaneously adding glucose units of maltose and sucrose [maltose + sucrose + α-1,4 glucan$_n$ = fructose + α-1,4 glucan$_{n+3}$] (Okada and Hehre, 1974; De Montalk *et al*., 1999). Such a storage polysaccharide would probably remain linear because *H. tiamatea* lacks any obvious glycogen branching and GH13 debranching enzyme (isoamylase). Recycling of the α-1,4-glucan could be mediated by concerted action of a GT35 glycogen phosphorylase and a GH77 α-1,4-glucanotransferase via glucose-1-phosphate to glucose-6-phosphate. Almost all respective enzymes are co-located in a single cluster in the *H. tiamatea* genome, which supports that they act together.

Halorhabdus tiamatea also possesses a trehalose synthase-like GH13 (HTIA_0926). Trehalose synthase (TreS) converts maltose to the non-reducing disaccharide trehalose, which can serve as additional storage compound, but is mainly known for its function as compatible solute. Presence of trehalose in *H. tiamatea* has already been hypothesized before (Antunes *et al*., 2011b) and corroborates recent findings that *Halobacteriales* not only use the salt-in, but also the organic osmolyte strategy, e.g. by internal accumulation of trehalose and glycine-betaine (Youssef *et al*., 2013).

It is noteworthy that in *H. tiamatea* storage compounds and osmoregulation are possibly interconnected, similarly as in species that use the alternate *TreY/TreZ* trehalose biosynthesis pathway such as *Sulfolobus* spp. (Avonce *et al*., 2006). In addition to trehalose, also maltose might play a dual role as precursor for both trehalose and a possible storage glucan. Thus, *H. tiamatea* could use storage glucan biosynthesis to regulate its pool of osmoregulating trehalose.

Habitat-specific adaptations

Halorhabdus tiamatea and *H. utahensis* exhibit some notable differences that are likely linked to their isolation sites. For example, the lack of pigmentation of *H. tiamatea* has been interpreted as adaptation to a light-deprived environment (Antunes *et al*., 2008a). *Halorhabdus tiamatea* features mercuric ion and arsenate reductases, which mirrors the specific ion compositions in Red Sea anoxic brine pools (Antunes *et al*., 2011a). *Halorhabdus tiamatea* also contains genes for the degradation of methylphosphonate that *H. utahensis* lacks (see Supporting Information Text). The Shaban Deep is a phosphate-limited environment (Antunes *et al*., 2011b), which favours species with alternative phosphorus acquisition strategies.

Halorhabdus tiamatea has sugar transporters with annotated specificities (ribose, xylulose, maltose and maltodextrin), whereas *H. utahensis* has been reported not to contain any known sugar transporter (Anderson *et al*., 2011). Likewise, *H. tiamatea* has the capacity to target a broader spectrum of polysaccharides than *H. utahensis*. Deep-sea habitats typically receive only little land plant, algal and seagrass carbohydrate substrates. Detritus sinking in from the photic zone will be largely consumed when it reaches the deep sea, and mostly the more recalcitrant components such as xylan and arabinan hemicelluloses, cellulose and connecting pectin will prevail. In case of DHALs, such compounds accumulate at the boundary layer of the seawater and the denser brine, and only little ultimately reaches the sediment. Hence, *H. tiamatea* is likely carbon limited in the Shaban Deep. In this context, the ability to store PHA and possibly α-1,4-glucans might be crucial for its survival. *Halorhabdus utahensis* in contrast stems from the sediment of the shallow Great Salt Lake of Utah. This lake has influxes from the Bear, Webber and Jordan Rivers, and thus features higher availabilities of suitable substrates.

One distinction of *H. tiamatea* from *H. utahensis* is its higher GH13 gene number (Table 2). *Halorhabdus tiamatea* has seven such genes (six of which were expressed) with functions that indicate (i) the degradation of exogenous α-glucans, (ii) the possible synthesis/turnover of a storage α-glucan and (iii) synthesis/turnover of trehalose. We found similarly high GH13 gene frequencies in *Hrd.* species that we enriched from the brine of another DHAL, the Mediterranean thalassohaline DHAL Medee (SW off the Western coast of Crete). Shotgun metagenomics of the enrichment (termed ANR26) yielded a 184 kbp contig carrying a 16S rRNA gene with 99.7% sequence identity to *H. tiamatea* (Fig. 1 and Supporting Information Text). Metagenome analyses demonstrated that the enrichment contained 80–95% *Hrd.* species and that its CAZyme profile correlated much better to *H. tiamatea* than to *H. utahensis* (Supporting Information Table S4 and Supporting Information Text).

Concluding remarks

Hypersaline habitats in general and DHALs in particular seem geographically isolated. Nonetheless, strains of *Haloquadratum walsbyi* with highly similar genomes have been isolated from salterns in Spain and Australia, indicating mechanisms for exchange (Dyall-Smith *et al*., 2011). Such exchange would also explain the highly similar genomes of *H. tiamatea* and *H. utahensis*. It is therefore possible that *H. tiamatea* has been transported to the Shaban Deep, but does not belong to its autochthonous microbial community. While *H. tiamatea* has a gene repertoire that is distinct from that of *H. utahensis* and allows survival in DHALs, its preference for micro-oxic conditions, its light-dependent enzymes as well as its relatively high optimum growth temperature are much more in line with life in the upper sediment of terrestrial shallow warm hypersaline lakes. Likewise, specialization of *H. tiamatea* on plant-derived polysaccharides contradicts preference for DHALs because these habitats receive only little such material. This would also explain why we found only barely detectable abundances of *Hrd.* species in Medee brine samples by catalysed reporter deposition fluorescence *in situ* hybridization with a novel *Hrd.*-specific probe (Supporting Information Fig. S4 and Supporting Information Text).

Genomic and functional data from the as yet investigated *Hrd.* members point towards an ecological niche that involves the capability to degrade complex polysaccharides. Recent identifications of *Hrd.* members in various other hypersaline habitats (see Supporting Information Text) might even suggest that *Hrd.* species occupy such a niche in many hypersaline habitats worldwide.

Experimental procedures

Sampling and sequencing of H. tiamatea

DNA was extracted from a *H. tiamatea* pure culture using the modified phenol-chloroform protocol (Urakawa *et al*., 2010) and subsequently sequenced on a 454 FLX Ti sequencer

(454 Life Sciences, Branford, CT, USA). Assembly of 461 818 reads with NEWBLER v. 2.3 yielded two scaffolds consisting of 87 contigs (3.1 Mbp). Fidelity Systems (Fidelity Systems, Gaithersburg, MD, USA) carried out gap closure: PHRED/PHRAP (Ewing and Green, 1998; Ewing *et al*., 1998) and CONSED (Gordon, 2003) were used for final assembly. Repeat mis-assemblies were corrected with DUPFINISHER (Han and Chain, 2006), and a single scaffold was generated and verified using 384 Sanger end-sequenced fosmids. Additional direct sequencing reactions were necessary for full closure (Malykh *et al*., 2004). Illumina reads (GA II; PE library, ~ 160 mio reads) were used to correct 454 base calling base errors. This provided 197× coverage of the chromosome and 311× coverage of the plasmid, with an error rate of less than 1:100 000. Sequences have been deposited at the European Nucleotide Archive with the accession numbers HF571520-HF571521.

Gene prediction and annotation

Gene prediction and annotation of protein-coding genes was done as described elsewhere (Mann *et al*., 2013). Ribosomal RNA genes were identified via BLAST searches (Altschul *et al*., 1997) against public nucleotide databases and transfer RNA genes using TRNASCAN-SE v. 1.21 (Lowe and Eddy, 1997). CRISPRs were identified with CRISPRFINDER (Grissa *et al*., 2007). Selected CAZymes from multi-functional CAZyme families were subjected to in-depth phylogenetic analyses to uncover their substrate specificities. For each family, a set of experimentally characterized proteins was selected and aligned with their *H. tiamatea* homologues using MAFFT (Katoh *et al*., 2002) with iterative refinement and the Blosum62 matrix. Phylogenetic trees were computed from these alignments using PHYML (Guindon and Gascuel, 2003) with 100 replicates for bootstrapping and annotations derived based on proximities to experimentally characterized proteins.

Glucosidase activity measurements and proteomics

Growth conditions. Halorhabdus tiamatea cultures were grown as described previously (Antunes *et al*., 2008a) in HBM liquid medium (*Halobacteria* medium; DSMZ (German Collection of Microorganisms and Cell Cultures, Braunschweig, Germany) medium 372) in 200 ml glass vials until an optical density (600 nm) of 0.1. For anoxic conditions, vials were filled with medium and subsequently incubated in sealed cylinders with an anoxic gas phase (80% N_2/20% CO_2) and anaerobic container system sachets (MBraun UNILab, Garching, Germany). For oxic conditions, the vials were filled to one quarter with medium and incubated in sealed cylinders with a gas phase with 2% and 5% oxygen respectively. Peptide solutions were obtained from all three conditions as described elsewhere (Yakimov *et al*., 2011). All subsequent measurements were carried out in triplicates.

Glycosidase activity measurements. Protein extracts (~ 0.23 mg ml^{-1}) were stored at −80°C until use. Activity was measured in 96-well plates using 18 *p*NP sugars (Sigma Chemical, St. Louis, MO, USA) and a BioTek Synergy HT spectrophotometer (BioTek, Highland Park, VT, USA) as described previously (Alcaide *et al*., 2012; Hernández *et al*., 2013). Reactions contained 4 μg total protein and 1 mg ml^{-1} substrate in a 20-mM HEPES buffer (pH 7, $T = 30$°C, final volume: 150 μl) with or without 3 M KCl. The release of *p*NP was measured at 410 nm in 1 min intervals for 130 min with derivatives of α-D-glucose, β-D-glucose, α-D-maltose, α-D-maltopentose, α-D-maltohexose, β-D-cellobiose, α-L-galactose, β-D-galactose, α-D-xylose, β-D-xylose, α-L-arabinopyranose, β-L-arabinopyranose, α-L-arabinofuranose, α-L-rhamnose, α-D-mannose, β-D-lactose, α-L-fucose and β-D-acetylglucuronide.

Protein digestion and tagging with iTRAQ-4-plex®. Peptide solutions (50 μg) were labelled for 2 h at room temperature with half a unit of iTRAQ Reagent Multi-plex kit (AB SCIEX, Foster City, CA, USA), previously reconstituted with 70 μl of ethanol. In the iTRAQ labelling, tags 114, 115 and 116 were used for 0%, 2% and 5% oxygen conditions respectively. Afterwards, labelled samples containing the same protein content were combined, and the labelling reaction was stopped by evaporation in a Speed Vac (Eppendorf, Madrid, Spain).

Peptide fractionation at basic pH and mass spectrometry analysis. The digested, labelled and pooled samples were studied by RP-LC-MALDI TOF/TOF MS as described elsewhere (Yakimov *et al*., 2011), using 150 μg of digested and labelled peptides and a Fortis C18 column, 100 mm × 2.1 mm, 5 μm (Fortis Technologies, Marl, Germany). In brief, a MALDI TOF/TOF 4800 mass spectrometer (AB SCIEX) was used for acquisition and processing of the peptides. The resulting raw peak lists of precursors and fragment ions were filtered and exported with ABI-Extractor (Peaks-Bioinformatics Solutions, Waterloo, ON, Canada). Protein identification and quantitation were done with MASCOT v. 2.3.01 (Matrix Science, London, UK) and PHENYX v. 2.6 (GeneBio, Geneva, Switzerland). The search was performed against the predicted protein sequences of *H. tiamatea*. The concatenated target-decoy database search strategy was used to estimate the false positive rate (below 1%) to improve reliability of the data (P-value < 0.01). A minimum of two unique peptides and three sets of spectra obtained in triplicated RP-LC-MALDI TOF/TOF MS data was required for protein identification and further quantification.

Acknowledgments

We thank the crew of the R/V *Urania* for sampling of the Medee DHAL, Jörg Wulf for catalysed reporter deposition fluorescence *in situ* hybridization analyses, Rafael Bargiela for helping with figures and Rudolf Amann for critical reading of the manuscript. This study was supported by the EU FP7 project MAMBA ('Marine Metagenomics for New Biotechnological Applications', FP7-KBBE-2008–226977; http://mamba.bangor.ac.uk/), the Spanish Ministry of Economy and Competitiveness (grant BIO2011–25012) and the Max Planck Society. H.T., O.V.G. and P.N.G. acknowledge the support of EU FP7 for the project MicroB3 (OCEAN-2011-287589).

References

Alcaide, M., Messina, E., Richter, M., Bargiela, R., Peplies, J., Huws, S.A., *et al*. (2012) Gene sets for utilization of

primary and secondary nutrition supplies in the distal gut of endangered Iberian lynx. *PLoS ONE* **7:** e51521.

Altschul, S.F., Madden, T.L., Schäffer, A.A., Zhang, J., Zhang, Z., Miller, W., *et al*. (1997) Gapped BLAST and PSI-BLAST: a new generation of protein database search programs. *Nucleic Acids Res* **25:** 3389–3402.

Anderson, I., Tindall, B.J., Pomrenke, H., Göker, M., Lapidus, A., Nolan, M., *et al*. (2009) Complete genome sequence of *Halorhabdus utahensis* type strain (AX-2^T). *Stand Genomic Sci* **1:** 218–225.

Anderson, I., Scheuner, C., Göker, M., Mavromatis, K., Hooper, S.D., Porat, I., *et al*. (2011) Novel insights into the diversity of catabolic metabolism from ten haloarchaeal genomes. *PLoS ONE* **6:** e20237.

Andrei, A.-Ş., Banciu, H.L., and Oren, A. (2012) Living with salt: metabolic and phylogenetic diversity of archaea inhabiting saline ecosystems. *FEMS Microbiol Lett* **330:** 1–9.

Antunes, A., Eder, W., Fareleira, P., Santos, H., and Huber, R. (2003) *Salinisphaera shabanensis* gen. nov., sp. nov., a novel, moderately halophilic bacterium from the brine-seawater interface of the Shaban Deep, Red Sea. *Extremophiles* **7:** 29–34.

Antunes, A., França, L., Rainey, F.A., Huber, R., Nobre, M.F., Edwards, K.J., *et al*. (2007) *Marinobacter salsuginis* sp. nov., isolated from the brine-seawater interface of the Shaban Deep, Red Sea. *Int J Syst Evol Microbiol* **57:** 1035–1040.

Antunes, A., Taborda, M., Huber, R., Moissl, C., Nobre, M.F., and da Costa, M.S. (2008a) *Halorhabdus tiamatea* sp. nov., a non-pigmented, extremely halophilic archaeon from a deep-sea, hypersaline anoxic basin of the Red Sea, and emended description of the genus *Halorhabdus*. *Int J Syst Evol Microbiol* **58:** 215–220.

Antunes, A., Rainey, F.A., Wanner, G., Taborda, M., Pätzold, J., Nobre, M.F., *et al*. (2008b) A new lineage of halophilic, wall-less, contractile bacteria from a brine-filled deep of the Red Sea. *J Bacteriol* **190:** 3580–3587.

Antunes, A., Ngugi, D.K., and Stingl, U. (2011a) Microbiology of the Red Sea (and other) deep-sea anoxic brine lakes. *Environ Microbiol Rep* **3:** 416–433.

Antunes, A., Alam, I., Bajic, V.B., and Stingl, U. (2011b) Genome sequence of *Halorhabdus tiamatea*, the first archaeon isolated from a deep-sea anoxic brine lake. *J Bacteriol* **193:** 4553–4554.

Avonce, N., Mendoza-Vargas, A., Morett, E., and Iturriaga, G. (2006) Insights on the evolution of trehalose biosynthesis. *BMC Evol Biol* **6:** 109.

Bortoluzzi, G., Borghini, M., La Cono, V., Genovese, L., Foraci, F., Polonia, A., *et al*. (2011) The exploration of deep hypersaline anoxic basins. Marine research at CNR – Marine Ecology: 95–108.

Cantarel, B.L., Coutinho, P.M., Rancurel, C., Bernard, T., Lombard, V., and Henrissat, B. (2009) The Carbohydrate-Active EnZymes database (CAZy): an expert resource for glycogenomics. *Nucleic Acids Res* **37:** D233–D238.

De Montalk, G.P., Remaud-Simeon, M., Willemot, R.M., Planchot, V., and Monsan, P. (1999) Sequence analysis of the gene encoding amylosucrase from *Neisseria polysaccharea* and characterization of the recombinant enzyme. *J Bacteriol* **181:** 375–381.

Dyall-Smith, M.L., Pfeiffer, F., Klee, K., Palm, P., Gross, K., Schuster, S.C., *et al*. (2011) *Haloquadratum walsbyi*: limited diversity in a global pond. *PLoS ONE* **6:** e20968.

Ewing, B., and Green, P. (1998) Base-calling of automated sequencer traces using phred. II. Error probabilities. *Genome Res* **8:** 186–194.

Ewing, B., Hiller, L., Wendt, M.C., and Green, P. (1998) Base-calling of automated sequencer traces using phred. I. Accuracy assessment. *Genome Res* **8:** 175–185.

Galinski, E.A. (1995) Osmoadaptation in bacteria. *Adv Microb Physiol* **37:** 272–328.

Gordon, D. (2003) Viewing and editing assembled sequences using Consed. *Curr Protoc Bioinformatics* **2:** 11.2.1–11.2.43.

Grissa, I., Vergnaud, G., and Pourcel, C. (2007) CRISPRFinder: a web tool to identify clustered regularly interspaced short palindromic repeats. *Nucleic Acids Res* **35:** W52–W57.

Guindon, S., and Gascuel, O. (2003) A simple, fast, and accurate algorithm to estimate large phylogenies by maximum likelihood. *Syst Biol* **52:** 696–704.

Han, C.S., and Chain, P. (2006) Finishing repetitive regions automatically with Dupfinisher. In *Proceedings of the 2006 International Conference on Bioinformatics and Computational Biology*. Arabnia, H.R. and Valafar, H. (eds). Las Vegas, NV, USA: CSREA Press, pp. 142–147.

Henrissat, B., and Coutinho, P.M. (2001) Classification of glycoside hydrolases and glycosyltransferases from hyperthermophiles. *Method Enzymol* **330:** 183–201.

Hernández, E., Bargiela, R., Diez, M.S., Friedrichs, A., Pérez-Cobas, A.E., Gosalbes, M.J., *et al*. (2013) Functional consequences of microbial shifts in the human gastrointestinal tract linked to antibiotic treatment and obesity. *Gut Microbes* **4:** 306–315.

Horie, A., Tomita, T., Saiki, A., Kono, H., Taka, H., Mineki, R., *et al*. (2009) Discovery of proteinaceous N-modification in lysine biosynthesis of *Thermus thermophilus*. *Nat Chem Biol* **5:** 673–679.

Itoh, T., Akao, S., Hashimoto, W., Mikami, B., and Murata, K. (2004) Crystal structure of unsaturated glucuronyl hydrolase, responsible for the degradation of glycosaminoglycan, from *Bacillus* sp. GL1 at 1.8 A resolution. *J Biol Chem* **279:** 31804–31812.

Jiao, N., Feng, F., and Wei, B. (2006) Proteorhodopsin – a new path for biological utilization of light energy in the sea. *Chin Sci Bull* **51:** 889–896.

Kather, B., Stingl, K., van der Rest, M.E., Altendorf, K., and Molenaar, D. (2000) Another unusual type of citric acid cycle enzyme in *Helicobacter pylori*: the malate:quinone oxidoreductase. *J Bacteriol* **182:** 3204–3209.

Katoh, K., Misawa, K., Kuma, K., and Miyata, T. (2002) MAFFT: a novel method for rapid multiple sequence alignment based on fast Fourier transform. *Nucleic Acids Res* **30:** 3059–3066.

Khotimchenko, Y., Khozhaenko, E., Kovalev, V., and Khotimchenko, M. (2012) Cerium binding activity of pectins isolated from the seagrasses *Zostera marina* and *Phyllospadix iwatensis*. *Mar Drugs* **10:** 834–848.

Kitaoka, M., Matsuoka, Y., Mori, K., Nishimoto, M., and Hayashi, K. (2012) Characterization of a bacterial

laminaribiose phosphorylase. *Biosci Biotechnol Biochem* **76:** 343–348.
Lombard, V., Golaconda Ramulu, H., Drula, E., Coutinho, P.M., and Henrissat, B. (2013) The carbohydrate-active enzymes database (CAZy) in 2014. *Nucleic Acids Res* **42:** D490–D495.
Lowe, T.M., and Eddy, S.R. (1997) tRNAscan-SE: a program for improved detection of transfer RNA genes in genomic sequence. *Nucleic Acids Res* **25:** 955–964.
Ma, K., Schicho, R.N., Kelly, R.M., and Adams, M.W.W. (1993) Hydrogenase of the hyperthermophile *Pyrococcus furiosus* is an elemental sulfur reductase or sulfhydrogenase: evidence for a sulfur-reducing hydrogenase ancestor. *Proc Natl Acad Sci USA* **90:** 5341–5344.
Ma, K., Weiss, R., and Adams, M.W.W. (2000) Characterization of hydrogenase II from the hyperthermophilic archaeon *Pyrococcus furiosus* and assessment of Its role in sulfur reduction. *J Bacteriol* **182:** 1864–1871.
Mai, X., and Adams, M.W.W. (1996) Characterization of a fourth type of 2-keto acid-oxidizing enzyme from a hyperthermophilic archaeon: 2-ketoglutarate ferredoxin oxidoreductase from *Thermococcus litoralis*. *J Bacteriol* **178:** 5890–5896.
Malykh, A., Malykh, O., Polushin, N., Kozyavkin, S., and Slesarev, A. (2004) Finishing 'Working Draft' BAC projects by directed sequencing with ThermoFidelase and Fimers. *Method Mol Biol* **255:** 295–308.
Mann, A.J., Hahnke, R.L., Huang, S., Werner, J., Xing, P., Barbeyron, T., *et al*. (2013) The genome of the alga-associated marine flavobacterium *Formosa agariphila* KMM3901^T reveals a broad potential for degradation of algal polysaccharides. *Appl Environ Microbiol* **79:** 6813–6822.
Martens, E.C., Lowe, E.C., Chiang, H., Pudlo, N.A., Wu, M., McNulty, N.P., *et al*. (2011) Recognition and degradation of plant cell wall polysaccharides by two human gut symbionts. *PLoS Biol* **9:** e1001221.
Murray, A.E., Kenig, F., Fritsen, C.H., McKay, C.P., Cawley, K.M., Edwards, R., *et al*. (2012) Microbial life at −13°C in the brine of an ice-sealed Antarctic lake. *Proc Natl Acad Sci USA* **109:** 20626–20631.
Nelson-Sathi, S., Dagan, T., Landan, G., Janssen, A., Steel, M., McInerney, J.O., *et al*. (2012) Acquisition of 1000 eubacterial genes physiologically transformed a methanogen at the origin of *Haloarchaea*. *Proc Natl Acad Sci USA* **109:** 20537–20542.
Ning, Z., Cox, A.J., and Mullikin, J.C. (2001) SSAHA: a fast search method for large DNA databases . *Genome Res* **11:** 1725–1729.
Okada, G., and Hehre, E.J. (1974) New Studies on amylosucrase, a bacterial alpha-D-glucosylase that directly converts sucrose to a glycogen-like alpha-glucan. *J Biol Chem* **249:** 126–135.
Oren, A. (1991) Anaerobic growth of halophilic archaeobacteria by reduction of fumarate. *J Gen Microbiol* **137:** 1387–1390.
Oren, A., and Gurevich, P. (1994) Production of D-lactate, acetate, and pyruvate from glycerol in communities of halophilic archaea in the Dead Sea and in saltern crystallizer ponds. *FEMS Microbiol Ecol* **14:** 147–155.
Oren, A., Vreeland, R.H., and Ventosa, A. (2007) International Committee on systematics of Prokaryotes; subcommittee on the taxonomy of *Halobacteriaceae* and subcommittee on the taxonomy of *Halomonadaceae*. *Int J Syst Evol Microbiol* **57:** 2975–2978.
Park, H.-W., Kim, S.-T., Sancar, A., and Deisenhofer, J. (1995) Crystal structure of DNA photolyase from *Escherichia coli*. *Science* **268:** 1866–1872.
Pautot, G., Guennoc, P., Coutelle, A., and Lyberis, N. (1984) Discovery of a large brine deep in the northern Red Sea. *Nature* **310:** 133–136.
Pilcher, R.S., and Blumstein, R.D. (2007) Brine volume and salt dissolution rates in Orca Basin, northeast Gulf of Mexico. *Am Assoc Pet Geol Bull* **91:** 823–833.
Popper, Z.A., Michel, G., Hervé, C., Domozych, D.S., Willats, W.G., Tuohy, M.G., *et al*. (2011) Evolution and diversity of plant cell walls: from algae to flowering plants. *Annu Rev Plant Biol* **62:** 567–590.
Rawls, K.S., Martin, J.H., and Maupin-Furlow, J.A. (2011) Activity and transcriptional regulation of bacterial protein-like glycerol-3-phosphate dehydrogenase of the haloarchaea in *Haloferax volcanii*. *J Bacteriol* **193:** 4469–4476.
Remelli, W., Guerrieri, N., Klodmann, J., Papenbrock, J., Pagani, S., and Forlani, F. (2012) Involvement of the *Azotobacter vinelandii* rhodanese-like protein RhdA in the glutathione regeneration pathway. *PLoS ONE* **7:** e45193.
Reusch, R.N., and Sadoff, H.L. (1988) Putative structure and functions of a poly-beta-hydroxybutyrate/calcium polyphosphate channel in bacterial plasma membranes. *Proc Natl Acad Sci USA* **85:** 4176–4180.
Rice, P., Longden, I., and Bleasby, A. (2000) EMBOSS: the European Molecular Biology Open Software Suite. *Trends Genet* **16:** 276–277.
Sakai, S., Takaki, Y., Shimamura, S., Sekine, M., Tajima, T., Kosugi, H., *et al*. (2011) Genome sequence of a mesophilic hydrogenotrophic methanogen *Methanocella paludicola*, the first cultivated representative of the order *Methanocellales*. *PLoS ONE* **6:** e22898.
Sakon, J., Irwin, D., Wilson, D.B., and Karplus, P.A. (1997) Structure and mechanism of endo/exocellulase E4 from *Thermomonospora fusca*. *Nat Struct Biol* **4:** 810–818.
Schryvers, A., and Weiner, J.H. (1981) The anaerobic sn-glycerol-3-phosphate dehydrogenase of *Escherichia coli*. *J Biol Chem* **256:** 9959–9965.
Stamatakis, A., Ludwig, T., and Meier, H. (2005) RAxML-III: a fast program for maximum likelihood-based inference of large phylogenetic trees. *Bioinformatics* **21:** 456–463.
Teeling, H., Waldmann, J., Lombardot, T., Bauer, M., and Glöckner, F. (2004) TETRA: a web-service and a stand-alone program for the analysis and comparison of tetranucleotide usage patterns in DNA sequences. *BMC Bioinformatics* **5:** 163.
Urakawa, H., Martens-Habbena, W., and Stahl, D.A. (2010) High abundance of ammonia-oxidizing archaea in coastal waters, determined using a modified DNA extraction method. *Appl Environ Microbiol* **76:** 2129–2135.
Wainø, M., and Ingvorsen, K. (2003) Production of beta-xylanase and beta-xylosidase by the extremely halophilic archaeon *Halorhabdus utahensis*. *Extremophiles* **7:** 87–93.

Wainø, M., Tindall, B.J., and Ingvorsen, K. (2000) *Halorhabdus utahensis* gen. nov., sp. nov., an aerobic, extremely halophilic member of the *Archaea* from Great Salt Lake, Utah. *Int J Syst Evol Microbiol* **50:** 183–190.

Yakimov, M.M., La Cono, V., Smedile, F., DeLuca, T.H., Juárez, S., Ciordia, S., *et al*. (2011) Contribution of crenarchaeal autotrophic ammonia oxidizers to the dark primary production in Tyrrhenian deep waters (Central Mediterranean Sea). *ISME J* **5:** 945–961.

Yernool, D.A., McCarthy, J.K., Eveleigh, D.E., and Bok, J.-D. (2000) Cloning and characterization of the glucooligosaccharide catabolic pathway beta-glucan glucohydrolase and cellobiose phosphorylase in the marine hyperthermophile *Thermotoga neapolitana*. *J Bacteriol* **182:** 5172–5179.

Youssef, N.H., Savage-Ashlock, K.N., McCully, A.L., Luedtke, B., Shaw, E.I., Hoff, W.D., *et al*. (2013) Trehalose/2-sulfotrehalose biosynthesis and glycine-betaine uptake are widely spread mechanisms for osmoadaptation in the *Halobacteriales*. *ISME J* doi:10.1038/ismej.2013.165.

Zaporozhets, T.S. (2003) Neutrophil activation by sea hydrobiont biopolymers. *Antibiot Khimioter* **48:** 3–7, (in Russian).

Zhang, T., Datta, S., Eichler, J., Ivanova, N., Axen, S.D., Kerfeld, C.A., *et al*. (2011) Identification of a haloalkaliphilic and thermostable cellulase with improved ionic liquid tolerance. *Green Chem* **13:** 2083–2090.

Supporting information

Additional Supporting Information may be found in the online version of this article at the publisher's web-site:

Supporting Information Text. Transporters; motility and chemotaxis; phosphonate utilization; fermentations; biotechnological aspects; *Hrd.* species in Medee; biogeographical aspects.

Fig. S1. Whole genome alignment between *H. utahensis* and *H. tiamatea*. The genome of *H. tiamatea* was split into 50 bp fragments and subsequently mapped on the *H. utahensis* with SSAHA2 v. 2.5 (Ning *et al*., 2001).

Fig. S2. Numbers of GHs in archaeal genomes according to the CAZyme database (Cantarel *et al*., 2009). From top to bottom: *Halorhabdus tiamatea* SARL4B^T, *Haloterrigena turkmenica* 4k^T, *Halorhabdus utahensis* AX-2^T, *Halopiger xanaduensis* SH-6^T, *Caldivirga maquilingensis* IC-167^T, *Ignisphaera aggregans* AQ1.S1^T, *Sulfolobus islandicus* REY15A^T, *Sulfolobus solfataricus* P2^T, *Sulfolobus islandicus* Y.N.15.51^T, *Sulfolobus islandicus* M.16.27^T.

Fig. S3. Unrooted phylogenetic tree of characterized GH13 family proteins and GH13 family proteins of *H. tiamatea* (see Supporting Information Table S3 for details). Sequences were aligned with MAFFT (Katoh *et al*., 2002), and the tree was computed with the program PhyML (Guindon and Gascuel, 2003). Numbers indicate the bootstrap values (100 replicates). Proteins from *H. tiamatea* are marked by black diamonds.

Fig. S4. Identification of *Hrd.* species in a sample from the Eastern Mediterranean DHAL Medee. A: DAPI staining; B: hybridization with the probe Halo178 and helper probes Halo178-h1 and Halo178-h2, showing typical pleomorphic cells of *Hrd.* species. Images were post-processed with AutoQuant X (A and B; MediaCybernetics, Inc., Rockville, MD, USA) and Imaris 7.4.0 (only B; Bitplane AG, Zurich, Switzerland).

Table S1. Annotations of all 50 glycoside hydrolases in *H. tiamatea*, including gene identifiers (locus tags), closest characterized homologues and EC numbers.

Table S2. Differentially expressed proteins of *H. tiamatea* grown on HBM liquid medium with 2% and 5% oxygen in the headspace compared with 0% oxygen. Protein annotations and their associated biological processes are shown. A shows 435 proteins unambiguously identified with at least two peptides. B shows 183 proteins identified with on one peptide. Protein identification and quantitation was conducted with MASCOT v. 2.3.01 (A contains protein and B peptide scores). Log_2 ratios of the relative protein/peptide abundances at 2% versus 0% oxygen and 5% versus 0% oxygen are shown.

Table S3. NCBI GenPept labels and accession numbers of the GH13 proteins that were used in the phylogenetic analysis.

Table S4. Glycoside hydrolases in the genomes of *H. utahensis* (according to the CAZy database as of 10 December 2013), *H. tiamatea* and the ANR26 enrichment from the Eastern Mediterranean DHAL Medee. The first number represents absolute counts, the number in parentheses the relative number per Mbp and the number in boldface reflects GHs detected in the proteome.